SEMIANNUAL STATUS REPORT No. 4

NASA GRANT NAG-1-566

SOUND PROPAGATION OVER UNEVEN GROUND AND IRREGULAR TOPOGRAPHY

Semiannual Report, August 1986 - February 1987

by

Yves H. Berthelot, James A. Kearns, Allan D. Pierce, and Geoffrey L. Main

School of Mechanical Engineering

Georgia Institute of Technology

Atlanta, Georgia 30332

Submitted to

National Aeronautics and Space Administration

Langley Research Center

Hampton, Virginia 23665

NASA Technical Officer:

John S. Preisser

Mail Stop 460A

February, 1987

TABLE OF CONTENTS

List of Figures

INTRODUCTION

The goal of this research is to develop theoretical, computational, and experimental techniques for predicting the effects of irregular topography on long range sound propagation in the atmosphere. Irregular topography here is understood to imply a ground surface that (1) is not idealizable as being perfectly flat or (2) that is not idealizable as having a constant specific acoustic impedance. The interest of this study focuses on circumstances where the propagation is similar to what might be expected for noise from low-altitude air vehicles flying over suburban or rural terrain, such that rays from the source arrive at angles close to grazing incidence.

The objectives of the project, the experimental facility, and the early progress up through August 1986 have been described in the three previous semiannual reports [1,2,3]. The present report discusses those activities and developments that have resulted during the period, August 1986 through February 1987.

PERSONNEL

In addition to A. D. Pierce and G. L. Main, a third faculty member, Yves H. Berthelot, and a graduate student, James Kearns, are presently working on the project. For the upcoming third year effort, Drs. Pierce, Main, and Berthelot will be co-principal investigators. During the past reporting period, Dr. Berthelot and Dr. Main have been supervising the experimental phase of the project and Allan Pierce has been working primarily on the theoretical aspects.

Tentative plans have been made for all of the personnel working on this project to visit NASA Langley Research Center on February 23, 1987, and to discuss complementary NASA and Georgia Tech research activities with the NASA technical officer, Dr. John Preisser, and his colleagues.

EXPERIMENTAL FACILITY

Modifications to Spark Source

The spark generator developed during the earlier phases of this project (see, for example, Figs. 4, 5, 6 of February 1986 status report) consisted of two tungsten electrodes held and aligned by a two-pronged plexiglas fork. A spark was generated across a 3 to 4 millimeter gap between the electrode points by a circuit consisting of a 5 to 10 kilowatt power supply, a 1 megaohm resistor, and a 0.05 μF capacitor, all in series. During the past reporting period, some modifications were made to this spark generation apparatus. These modifications were intended to make the acoustic signal have a cleaner, less ragged, form, and to make it more nearly repeatable from run to run. One problem was that the acoustic pressure signal trace generated by the spark exhibited a "ringing" at times immediately following the initial pressure rise. The magnitude of the Fourier transform of the direct wave's acoustic pressure signal was somewhat erratic in form and it was suspected that this was associated with the "ringing" in the plot of acoustic pressure versus time.

One hypothesis was that the ringing was caused by an oscillation in the plasma generated by the spark discharge and that it would be partly eliminated if the discharge occurred at a lower voltage. The characteristic time associated with the pressure waveform was observed to depend in major part on the gap size; the larger the gap, the lower the dominant frequencies in the acoustic signal. However, the voltage required to break down (ionize) the air in the gap, so a spark could jump across, became larger when the gap size was increased. Typically, we found that 4 to 5 kilovolts was required before the air broke down when the gap sizes corresponded to dominant frequencies of interest. However, we also believed that, once the breakdown occured, a much lower voltage would suffice to drive current across the electrodes. Consequently, it might be better if one could somehow uncouple the processes of creating the breakdown and of generating current flow across the gap.

Another observation was that the electrodes were of a diameter comparable with the wavelength of the generated sound, and that the sound generated within the gap would partially be reflected by the electrodes and the electrode faces. Such reflections would interfere with the incident wave, and the time delay after first arrival of these reflected arrivals would be far too short to be gated out in time. An interference pattern resulting from such reflections is apparent in Figs. 4, 6, 8 of the August 1986 status report.

The modifications to the spark source (Fig. 1) incorporate certain features that are present in an apparatus designed by Dr. Mendel Kleiner at Chalmers Institute of Technology, and which

was recently used in similar experiments by Almgren [4]. The new electrodes are approximately 1/16" in diameter and made from stainless steel welding rods. The ductility of the stainless steel rods enables them to be shaped into a more desirable configuration. (Such was not possible with the previous tungsten rods.) This eliminates the need for the plexiglas fork support. Previously, the plexiglas fork was responsible for supporting and holding the tungsten rods in a desired configuration. In the new design, two stainless steel rods run parallel out of a wedged support block for approximately 6" and then bend through right angles, so that the two pointed ends come close together, but with a small gap. The gap size used in our experiments is of the order of 1 to 2 millimeters. These two rods are the "high" power, "low" voltage electrodes. A third rod mounted in the support block approaches the gap at an angle of 15 degrees from the plane containing the first two rods. This rod is a "low" power, "high" voltage trigger. Its point rests near the center of the gap and its projection on the previously mentioned plane bisects the other two electrodes.

The two bent electrodes that are separated by a gap transmit the charge stored in the 0.05 μF capacitor. The discharge is initiated when the trigger ionizes the gap with a 10 to 15 kV pulse. This pulse is generated by an automobile ignition coil. The trigger is able to induce the discharge across the other two electrodes at initial gap voltages (of the order of 2 kV) much lower than those required for spontaneous discharge. A sample of typical acoustic pressure waveforms generated by the new spark mechanism at various initial spark gap voltages is shown in Fig. 2. These figures show that there is a distinct decrease in "ringing" when the initial spark gap voltage decreases. Based on such tests, the decision was made to use a relatively low initial gap voltage of 2 kV in all of the subsequent experiments. Typical peak acoustic pressures at a distance of the order of 1 meter for the circumstances just described are of the order of 120 to 130 Pascals. Typical rise times (after passing the signal through a low-pass digital filter as described further below) and characteristic pulse duration times are of the order of 10 μs and 42 μs, respectively.

Ideally, the acoustic radiation from the spark should be repeatable from run to run and omnidirectional. However, since the data analysis method used in the present experiments depends only on the ratios of Fourier transforms of pressure waveforms at two microphone locations, one needs only test that such ratios are repeatable. With the reference microphone and the field microphone both at fixed (not necessarily equal) radial distances from the source, the omnidirectionality would be sufficient if the ratio of Fourier transforms were nearly independent of the direction from the source to the field microphone.

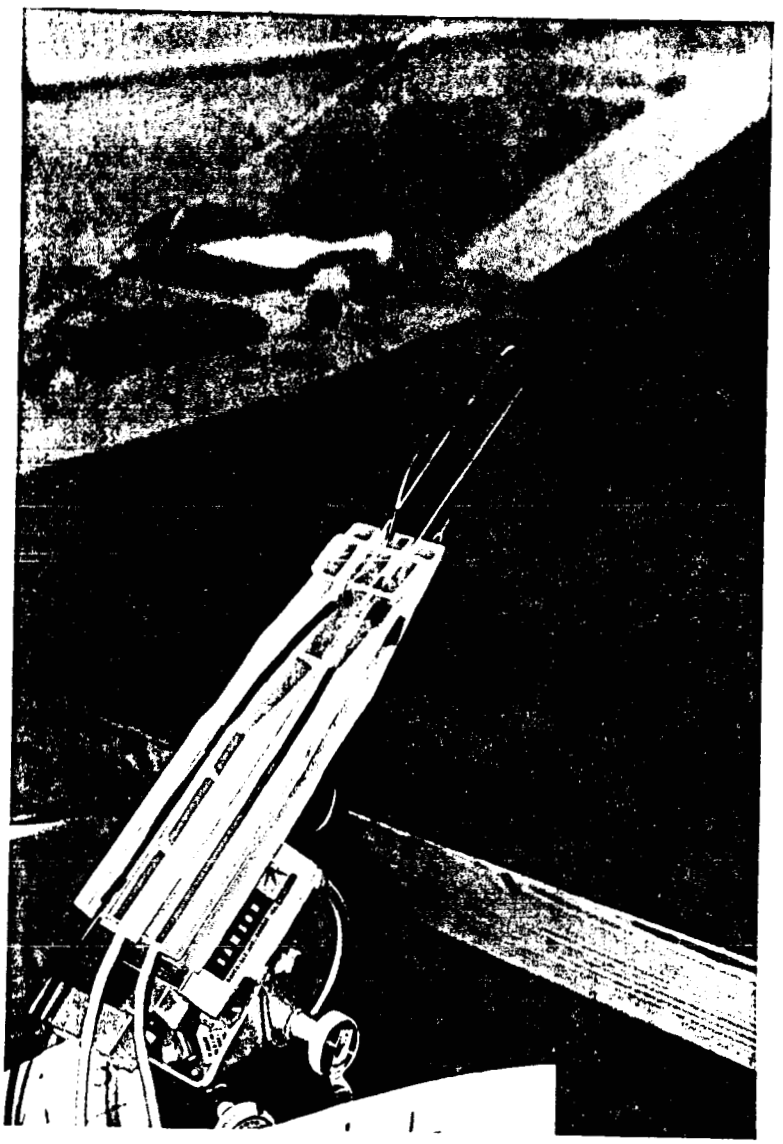

Figure 1. Photograph of the new design of the spark source, with two bent stainless steel electrodes separated by a gap and with a trigger electrode between them.

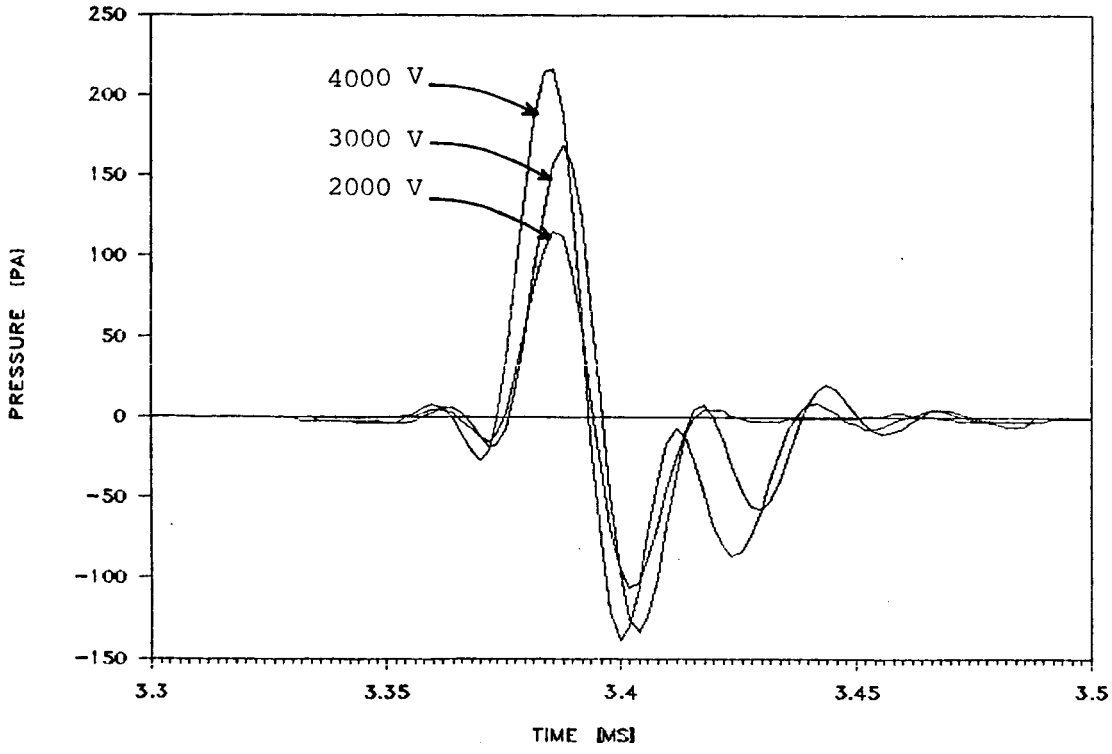

Figure 2. Acoustic pressure in pascals versus time in milliseconds at a range of 1.16 from the spark source. The lowest, middle and highest amplitude curves correspond to initial spark gap voltages of 2 kV, 3 kV, and 4 kV, respectively.

Eight trials (Fig. 3) were run with fixed field and reference microphone positions to test repeatability of the measurement of Fourier transform ratios. To test for omnidirectionality (Fig. 4), waveforms were recorded in seven successive trials with the direction from source to field microphone being different in each trial. For each such trial, the reference microphone waveform used in the data analysis was the same as was recorded in that trial. The reference microphone and its position were the same for all trials. The direct acoustic pathlengths were approximately equal for each microphone as well. The repeatability data was taken at the same height as the source while the directionality data was taken every 6 degrees over a range of -12 to 24 degrees from the horizontal. The reference microphone was located approximately 1.2 m from the source at an angle of roughly 35 degrees from the horizontal. The procedure consisted of dividing the Fourier transform of the field microphone pressure transient by the Fourier transform of the reference microphone pressure transient for several selected frequencies. The extent to which these ratios are independent of angle indicates the extent to which the source is omnidirectional. The tests indicate that, in general, the measurement of the ratio of Fourier transforms is accurate and reproducible to within 1/2 dB at all angles of interest in the vertical centerline plane for a frequency range of 5 to 35 kHz.

Suspension of Microphones

The position of the reference microphone was chosen such that the sound arriving at it during the time interval associated with the direct wave arrival be as close to free field (no reflected arrivals during the same time interval) measurements as possible and such that the microphone casing and suspension not impede or interfere with propagation of the acoustic wave to the field microphone. The reference microphone is suspended at a height roughly three times the height of the ridge (32.4 cm) by three separate lines of 1/16" nylon cord (Fig. 5). One of these cords traverses the width of the laboratory room at a height of 1 m above the table top. This cord suspends the reference microphone at that height. The other two cords attach to the front and rear of a thin aluminum shim upon which the microphone and pre-amp rest. These cords run from the shim to moorings on both sides of the table. The cords form a triangular window through which the incident wave travels before reaching the ridge and farfield. Any path length that extends from the source to one of these three cords and then to the field microphone is sufficient long enough to be gated out in time. No other supporting structures aside from the field microphone positioner (Fig. 6) are located such that they could cause scattered waves to

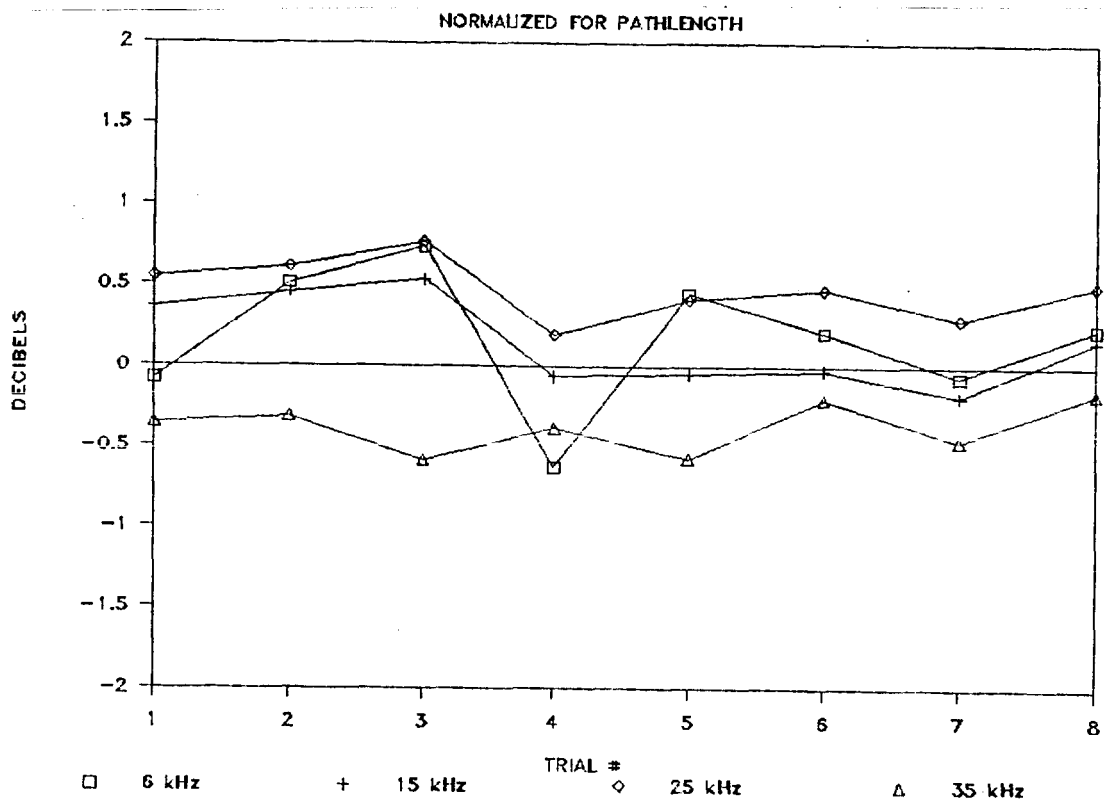

Figure 3. Experimental verification that the two microphone technique yields Fourier transform ratios that are the same in successive trials for the same conditions. For a given trial number (horizontal axis), the four curves correspond to ratios (expressed in dB) of the Fourier transforms at frequencies of 5 kHz (□), 15 kHz (+), 25 kHz (◇), and 35 kHz (△). The two microphones are at ranges of 1.06 and 0.96 m, respectively, and at angles of 35° and 0°, respectively.

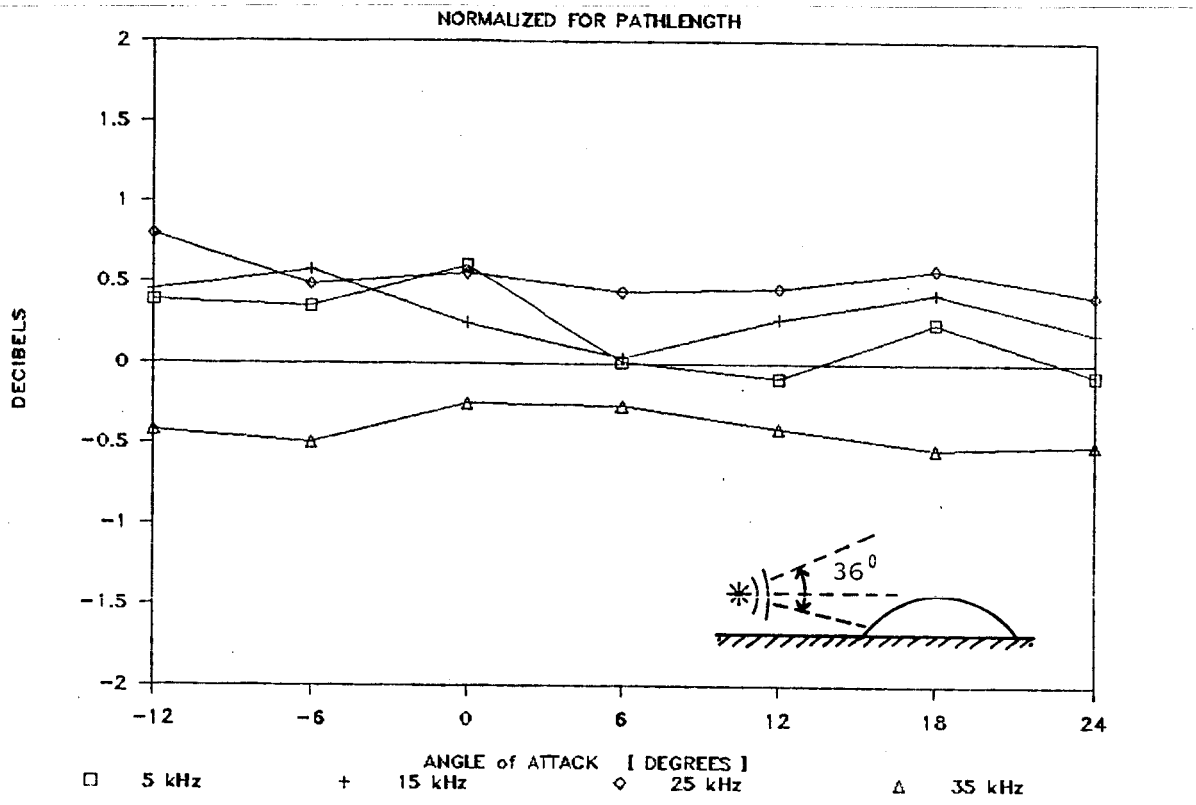

Figure 4. Experimental test of the omnidirectionality of the spark source. In each experiment the reference microphone and the field microphone are both at fixed ranges of the order of 1.16 m; the field microphone is slightly closer; the reference microphone is at $\theta_1 = 35^o$ with respect to the horizontal ray from the source, while the second microphone is at angle θ_2, denoted by "angle of attack" in the legend and varying from -12° to 24°. Vertical scale corresponds to ratio (expressed in dB) of the Fourier transform at the field microphone to that at the reference microphone. For a given field microphone angular position (horizontal axis), the four curves correspond to ratios of the Fourier transforms at frequencies of 5 kHz (□), 15 kHz (+), 25 kHz (◇), and 35 kHz (Δ).

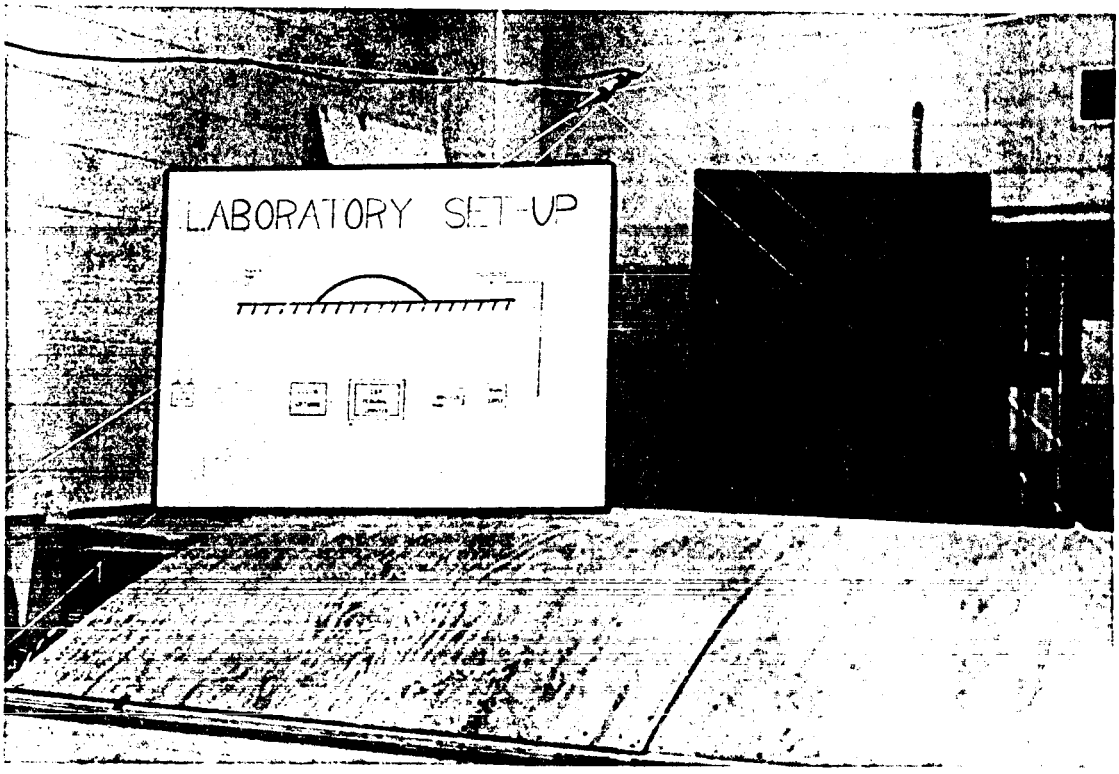

Figure 5. Photograph showing the method of support and a typical position of the reference microphone relative to that of the model terrain table.

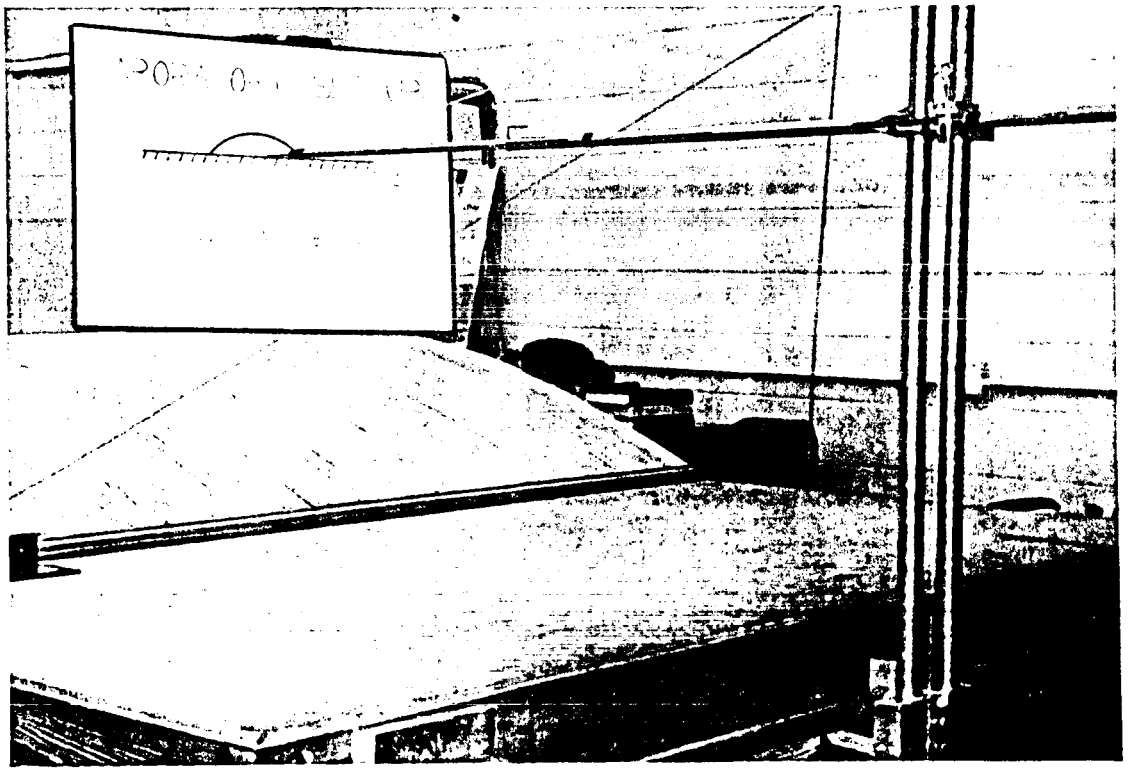

Figure 6. Photograph showing the method of support and a typical position of the field microphone relative to that of the model terrain table.

arrive at the field microphone during the same time interval as that of the dominant arrivals of interest in our experiments.

EXPERIMENTAL RESULTS

The experimental studies carried out or initiated during the period September 1986 through January 1987 fall into three categories. One was for acoustic propagation over the flat table top with both microphones sufficiently high above the table that reflected arrivals from the table surface should be gated out in time and therefore eliminated from the analysis. These free-field experiments enable one to eximine spreading loss, dissipation, and nonlinear effects. They also allow some examination of the extent to which the source per sé is affected by the proximity of the table. A second category of experiments is with a flat table top (no ridge present) and is intended for the measurement of the impedance of theflat surface at the point of reflection and for the study of how this impedance depends on the angle of incidence. Such experiments have been initiated relatively recently and the results are still being checked for consistency, so no actual results for surface impedance measurements are reported in the present progress report. The third category of experiments is with the curved ridge present on the table top and is intended to examine the effects (reflection, scattering, and diffraction) of this ridge on the propagation of sound.

General Procedure

The general experimental procedure is similar for all of the experiments reported here As is discussed in the February 1986 status report (see, for example, Fig. 1 in that report), the experimental system uses two 1/4" condenser microphones (B&K 4136), one at a reference point, and the other at a given field point. With obvious time interval selection, the transient pressure waveform recorded by the first microphone should contain no echoes from solid surfaces. The time windows during which data is captured are the same for both microphones. The two corresponding analog voltage signals that are output from the preamplifiers are amplified, sampled at intervals of 0.04 μs, and digitized to 12 bit precision. A constant is automatically added to each data sample such that the tabulation approximately begins and ends with values near zero. Since the voltage increment registered by a microphone is opposite in sign to that of the corresponding pressure increment, the sign of the shifted digitized data is reversed. Then the

data sets are filtered by a lowpass digital filter with an upper cutoff frequency of 50 kHz. The experimenter examines the resulting waveforms on a video screen and selects a time window for each of them, and for which Fourier transforms are to be calculated. The two time windows have the same duration (usually, 500 times 0.04 μs), but usually not the same time beginnings. The experimenter selects the waveform portion in these windows that he believes to be of interest and representative to what would be received if there were no undesired reflections contaminating the data. Data points outside these portions are then replaced by zeroes. In this way, two "windows" containing a reference microphone waveform and a field microphone waveform, respectively, are generated. The replacement of the extra data points by zeroes is in accord with the expectation that an acoustic pulse has negligible residual affect on the ambient pressure, and that the acoustic pressure before and after each waveform should ideally be zero. Small oscillating data values at the beginning and termination of each window's record are attributed to noise. The computed Fourier transform is treated and interpreted as if the value of the acoustic pressure were identically zero before the start of the window and after the end of the window.

The Fourier transform algorithm used in the subsequent calculations has been keyed-in from a listing (which had been circulating at Georgia Tech for considerable time, but whose actual origin is unknown) of a Fortran program developed by Norman Brenner and Charles Rader of MIT Lincoln Laboratory circa 1967 and which, according to the comment statements included with the listing, has some relationship to what is described in a paper "Fast Fourier transforms for fun and profit," by W. Gentleman and G. Sande, presented at the 1966 Fall Joint Computer Conference. For the circumstances for which the program is used in the present project, the program returns a set of N numbers $q(n)$ from an input set $v(n)$ according to the equation

$$q(n) = \sum_{m=1}^{N} v(m) e^{i2\pi(n-1)(m-1)/N}$$

Thus, if

$$v(n) = Kp(t_o + [n-1]\Delta t$$

then

$$q(m) \approx \frac{K}{\Delta t} e^{-i2\pi f_m t_o} \int_{-\infty}^{\infty} p(t) e^{i2\pi f_m t}\, dt$$

where

$$f_m = \frac{(m-1)}{N\Delta t} \quad \text{for } 1 < m < \frac{1}{2}N$$

Consequently, the value of the Fourier transform can be identified it one knows the time t_o at the start of the record, the number N of samples, the sampling interval Δt, and the apparent transduction constant K (volts per pascal).

Free-Field Experiments

A series of experiments were carried out to examine the dependence of the magnitude of the Fourier transform ratio on the radial distance of the field microphone from the source, with the position of the reference microphone held fixed. Measurements were taken at 5 different field microphone locations above the flat table top. All of the measurements were taken along the table centerline and at the same height as the source. Figure 7 gives an indication of how the amplitude corresponding to a given frequency drops off with increasing radial distance from the source. What is actually plotted is free field range dependence of the ratio (expressed in dB) of the Fourier transform of the pressure waveform at the field microphone to that at the reference microphone for two frequencies. The position of the range microphone is fixed at a rangle of approximately 1.16m, while the range of the field microphone varies from 2.5m to 8.5 m. The data is normalized (shifted by the same dB increment for each sample) to 0 dB at 2.57m. The upper and lower curves correspond to frequencies of 5 kHz and 25 kHz, respectively. A fitting of a straight line to each of these curves indicates that the drop in amplitude is somewhat larger (of ther order of 1 additional dB per doubling of distance) than the 6 dB per doubling of distance associated with spherical spreading. Preliminary estimates suggest that the discrepancy is too large to be accounted for by the known absorption of sound in air, but this conclusion needs further examination. For the present, we are using the experimentally derived attenuation laws whenever we wish to extrapolate data measured at one propagation path length to predict what would be measured at another propagation path length.

Examination of waveforms (although after passage through the low pass digital filter) does not indicate that nonlinear effects are significant for propagation between the ranges of 1 and 3.5 m. Figures 8 and 9 show free field (unaffected by the presence of the table) acoustic pressure waveforms that have been taken when the source to microphone distances are 120 cm and 260 cm, respectively. The judgement concerning the apparent absence of nonlinear affects is based on a qualitative comparison of the shapes of such waveforms, although no detailed quantitative examination has yet been carried out to substantiate this. The fact that the waveforms have been passed through a low-pass digital filter before examination may have suppressed well-known nonlinear effects such as steeping of waveforms.

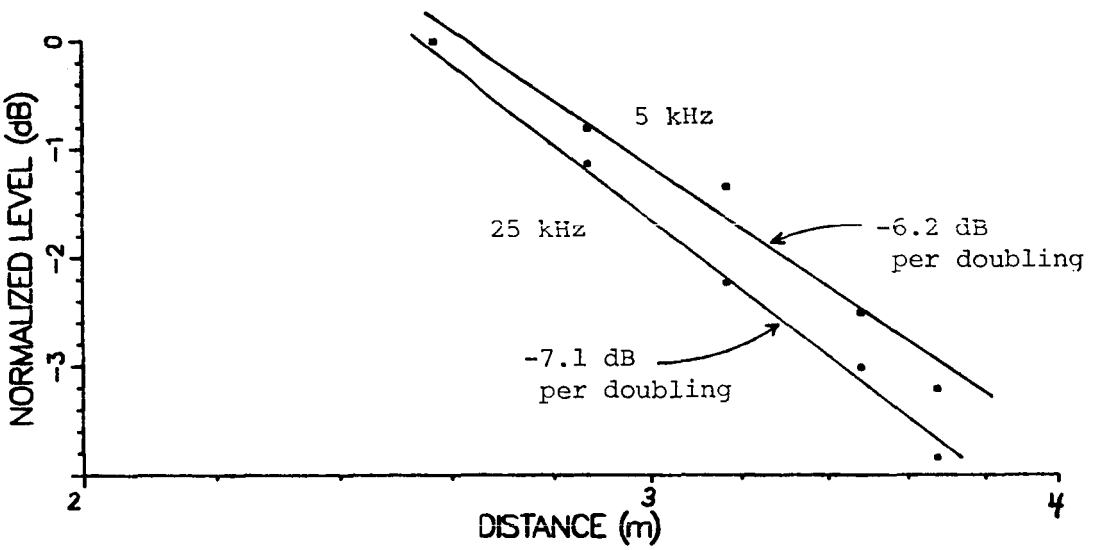

Figure 7. Free field range dependence of the ratio (expressed in dB) of the Fourier transform of the pressure waveform at the field microphone to that at the reference microphone. The position of the range microphone is fixed at a rangle of approximately 1.16m, while the range of the field microphone varies from 2.5m to 8.5 m. The data is normalized (shifted by the same dB increment for each sample) to 0 dB at 2.57m. The upper and lower curves correspond to frequencies of 5 kHz and 25 kHz, respectively.

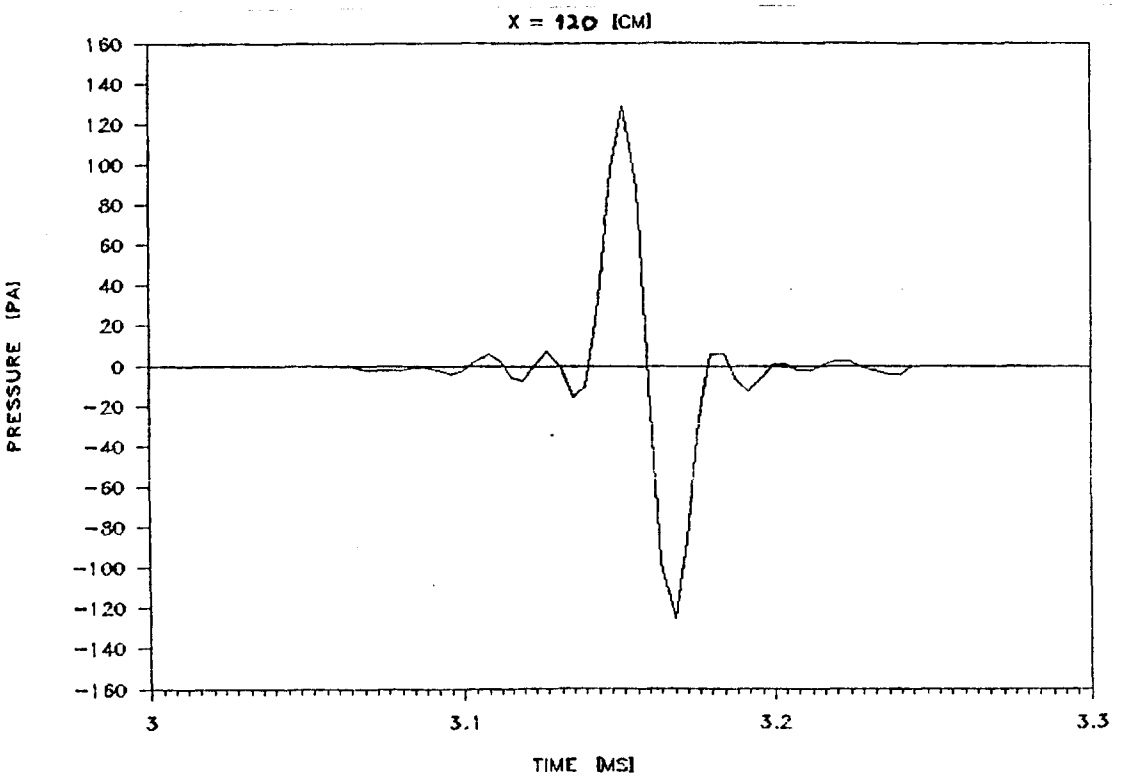

Figure 8. Recorded acoustic pressure waveform after passing digitized signal through a low-pass digital filter. This is a free field (unaffected by the presence of the table) waveform and is measured at a source to microphone distance of 120 cm. The precursor before the dominant pressure peak is believed to be an artifact of the digital filtering.

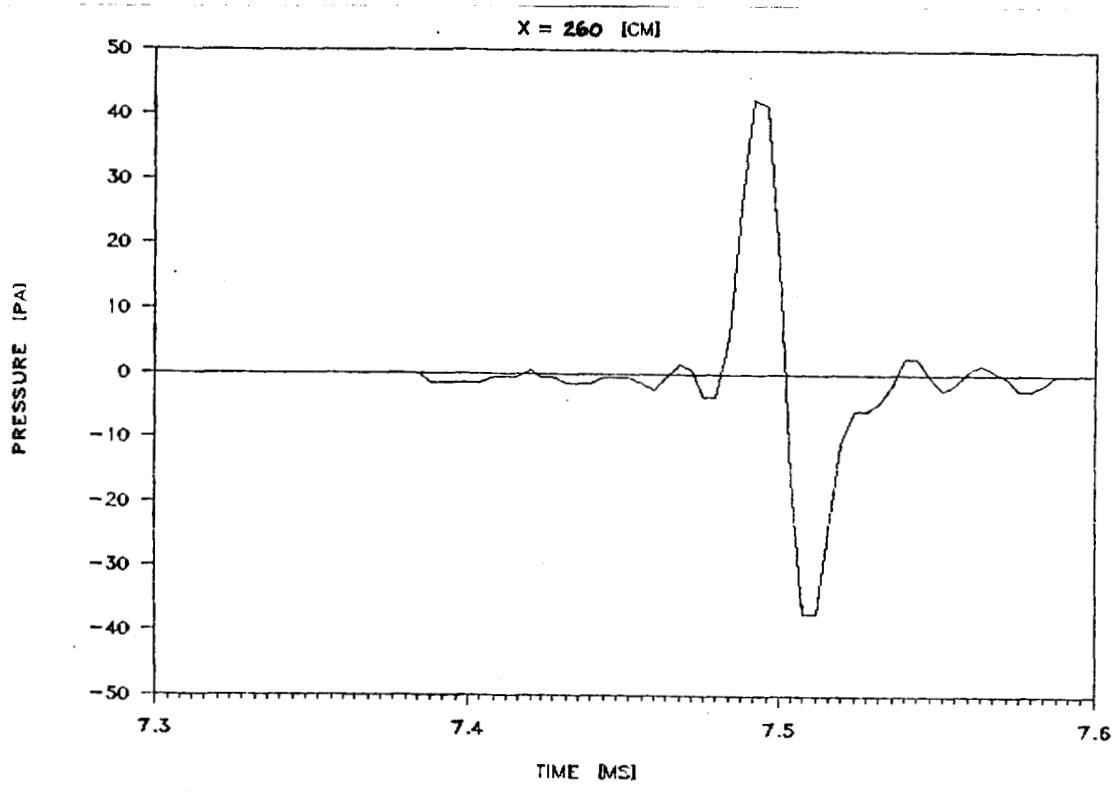

Figure 9. Recorded acoustic pressure waveform after passing digitized signal through a low-pass digital filter. This is a free field (unaffected by the presence of the table) waveform and is measured at a source to microphone distance of 260 cm. The precursor before the dominant pressure peak is believed to be an artifact of the digital filtering.

In a separate set of experiments, the direct wave pressure trace (as contrasted to the reflected wave) at a fixed radial distance was examined to see if there was any variation associated with the height of the source above the table top. No dscernible significant variation in amplitude, rise time or duration of the waveform was noticed for heights between 20 and 45 cm .

Experiments to Measure Acoustic Impedance

Another type of experiment which we have recently begun concerns the measurement of the acoustic impedance of the table top surface. The technique which we are using is sketched in Fig. 10. The spark source is at a height H_S above a flat plane. Sound reaches the microphone along direct (distance R_1) and reflected (net distance R_2) paths. Because the source is transient and because the path length difference $R_2 - R_1$ is sufficiently great, the two arrivals are separated in time. With appropriate correction for spherical spreading and with appropriate time shifts, one can deduce the incident and reflected waveforms at the reflection point. The ratio of Fourier transforms will then yield the reflection coefficient and, with additional calculation, one determines the impedance.

We chose this transient pulse method of measuring surface impedance because it makes use of equipment that we already have at hand. The principal difficulty in implementing this method is that the pathlength differences must be large enough to gate out the direct from reflected signals but also small enough to be measured accurately. Presently, we are using a single-microphone technique, but a double-microphone technique is also possible in which one does not have to have direct and reflected waveforms clearly separated in time. Our tentative reason for using the single microphone technique was so that one would not have to correct for phase shift and amplitude response versus frequency properties of the two microphones. However, the data taken to date shows strange anomalies in reflection coefficient versus frequency, which we doubt are real; so the technique either needs further refinement or else should be modified.

Insertion Loss Measurements

An extensive set of experiments have been carried out to determine how the presence of the ridge on the table affects the amplitude of sound at a given frequency. What is being measured is the ratio of the Fourier transform of the transient pressure waveform at a given point to what one would expect to have if the ridge were not present. Expressed in decibels, what is measured is what is commonly referred to as insertion loss in the literature. These measurements are of special

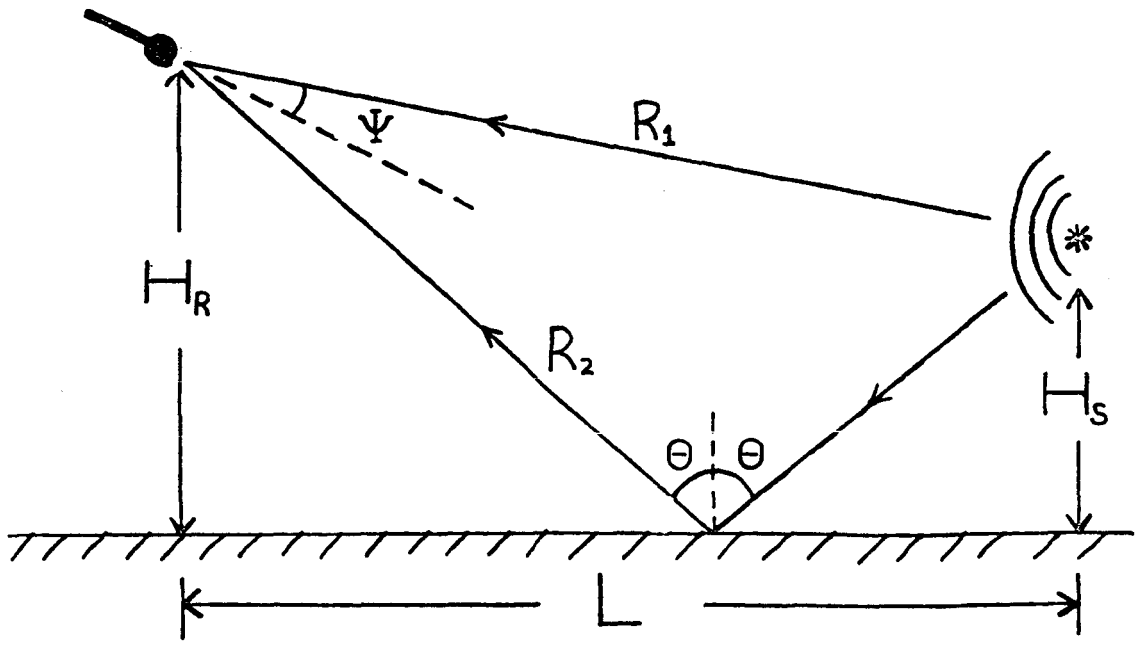

Figure 10. Sketch illustrating method with which surface impedances are tentatively being measured. The spark source is at a height H_S above a flat plane. Sound reaches the microphone along direct (distance R_1) and reflected (net distance R_2) paths. Because the source is transient and because the path length difference $R_2 - R_1$ is sufficiently great, the two arrivals are separated in time. With appropriate correction for spherical spreading and with appropriate time shifts, one can deduce the incident and reflected waveforms at the reflection point. The ratio of Fourier transforms will then yield the reflection coefficient and, with additional calculation, one determines the impedance.

interest as we have previously developed a theory (described in previous semiannual reports) for predicting their values. The comparison of theory with experiment is still in progress, but the results so far are encouraging.

Figure 11 gives the insertion loss on the surface of the ridge as a function of the arc length s in centimeters; the point $s = 0$ corresponds to the top of the ridge and smaller values of s correspond to points closer to the source. The three curves correspond to frequencies of 5 kHz (□), 15 kHz (+), and 25 kHz (◇). The source is at a net distance of 243.7 cm from the top of the ridge and at the same height. To tentatively check the extent to which this data corroborates with theory, we compare the data with what would be predicted for the case when a plane wave is indendent and the surface of the ridge is taken as rigid. The theory for such circumstances predicts that the insertion loss, regardless of the frequency (given that it is sufficiently high) should be a function of a dimensionless arc length ξ, where

$$\xi = \frac{s}{R}(kR/2)^{1/3}$$

Here $k = 2\pi f/c$, where f is frequency in Hertz, and c is the speed of sound. The quantity R is the radius (approximately 2.5 m) of curvature of the ridge at its top. Although the proportionality between ξ and s depends on frequency, the hard surface version of the theory predicts that the insertion loss depends on frequency only through the dependence of ξ on frequency.

Figure 12 replots the data of Fig. 11 in terms of insertion loss versus the dimensionless arclength parameter ξ. One may note that there is a substantial collapse in the three curves and that, moveover, all three experimental curves are relatively close to what is predicted by the theory. At present the anomalous behavior of the data at larger negative value of ξ, where the theory predicts an asymptotically constant insertion loss of -6 dB is not understood.

Figure 13 gives insertion loss above the apex ($x = 0$) of the ridge as a function of the height (y) in centimeters above the grazing plane. The two sets of data, which for simplicity, are connected by straight lines in the plotting, correspond to frequencies of 5 kHz (□) and 15 kHz (+). Figure 14 is for similar circumstances, only the horizontal coordinate x is at an intermediate distance (63.5 cm) on the shadow side. In Fig. 15, the coordinate x is at a relatively large distance of 209 cm. In the latter plot, we expect the results to tend to agree with the results of the knife edge diffraction theory, but the carrying out of the detailed comparison has yet to be performed.

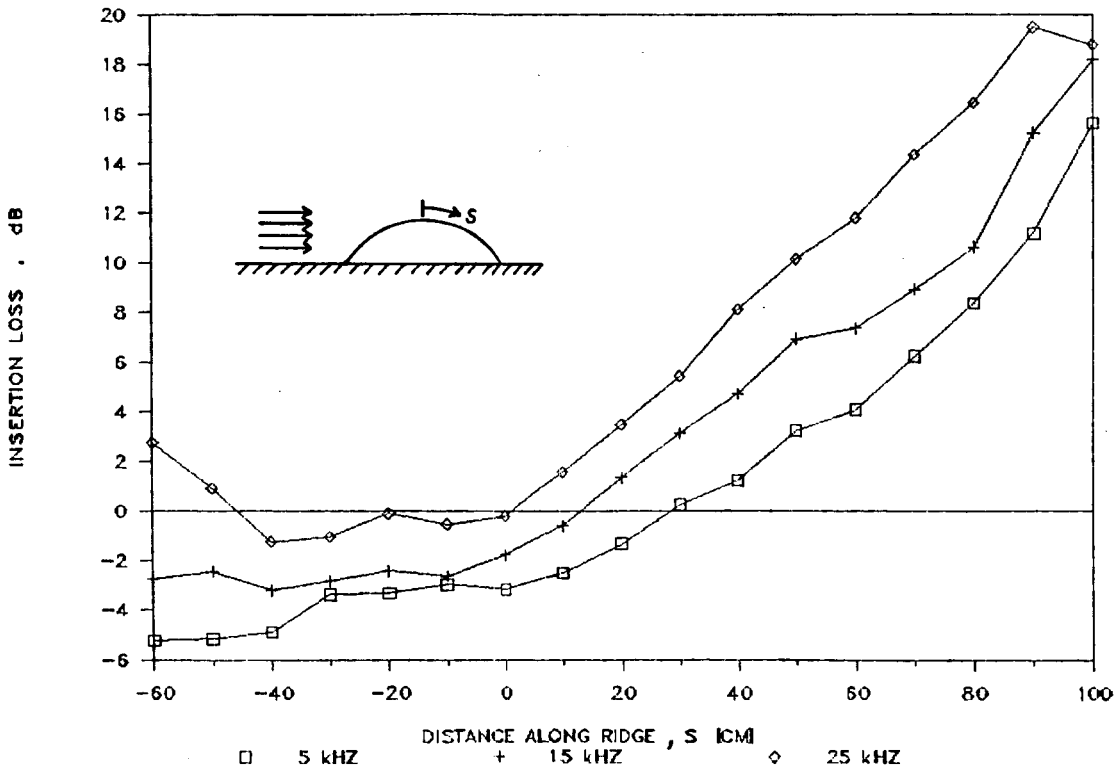

Figure 11. Insertion loss on the surface of the ridge as a function of the arc length s in centimeters; the point $s = 0$ corresponds to the top of the ridge and smaller values of s correspond to points closer to the source. The three curves correspond to frequencies of 5 kHz (□), 15 kHz (+), and 25 kHz (◇). The source is at a net distance of 243.7 cm from the top of the ridge and at the same height.

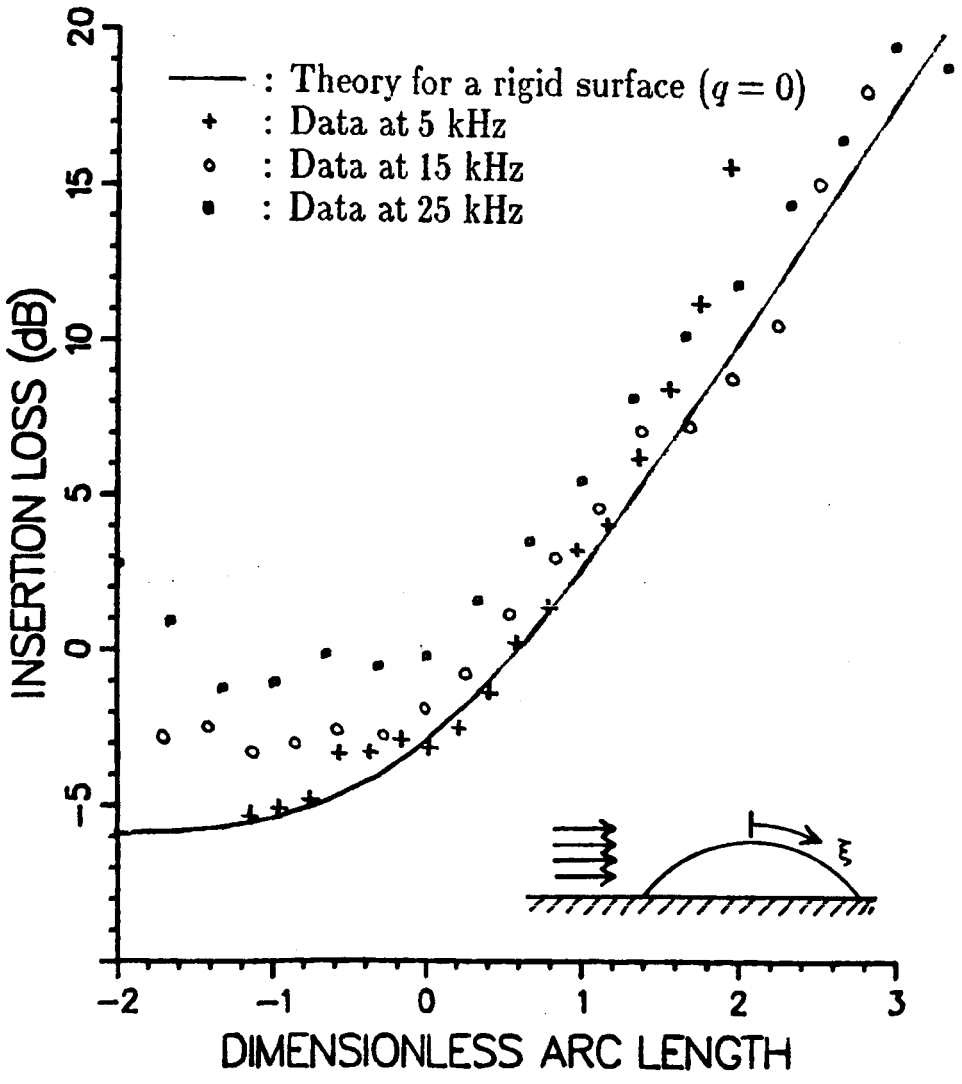

Figure 12. Replotting of data of Fig. 11 in terms of insertion loss versus the dimensionless arclength parameter ξ. One may note that there is a substantial collapse in the three curves and that, moveover, all three experimental curves are relatively close to what is predicted by the theory. At present the anomalous behavior of the data at larger negative value of ξ, where the theory predicts an asymptotically constant insertion loss of −6 dB is not understood.

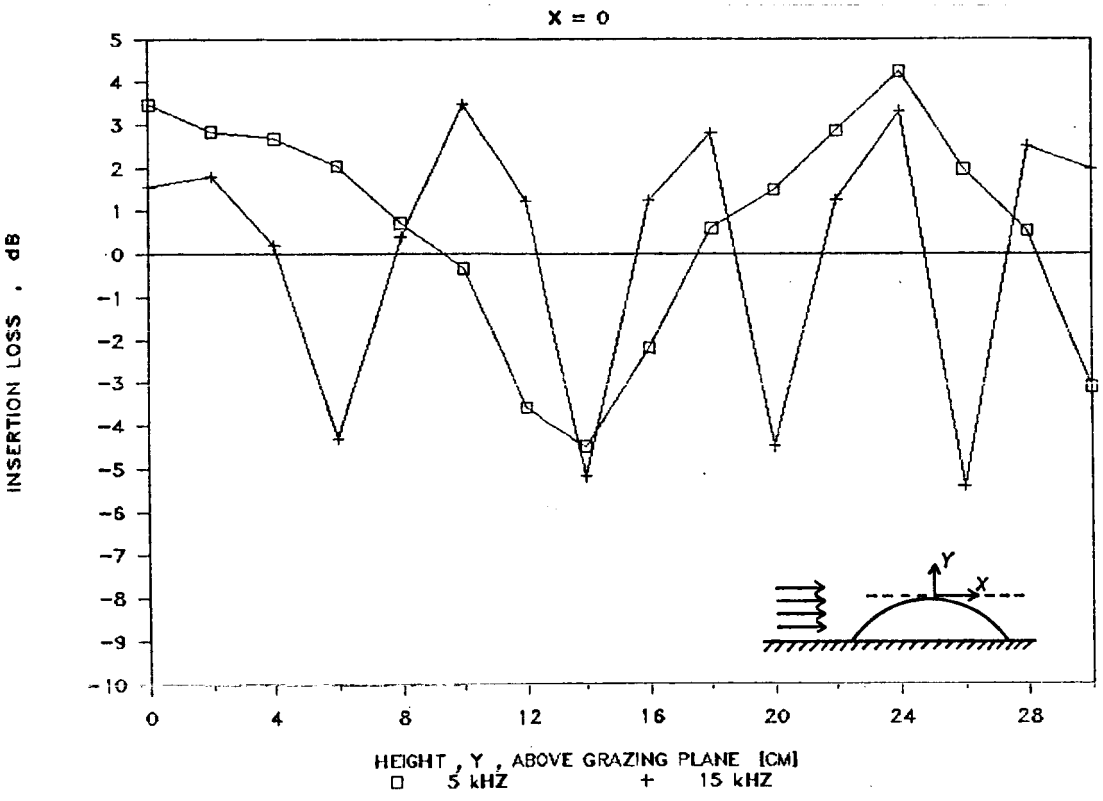

Figure 13. Insertion loss above the apex ($x = 0$) of the ridge as a function of the height (y) in centimeters above the grazing plane. The two sets of data, which for simplicity, are connected by straight lines in the plotting, correspond to frequencies of 5 kHz (□) and 15 kHz (+).

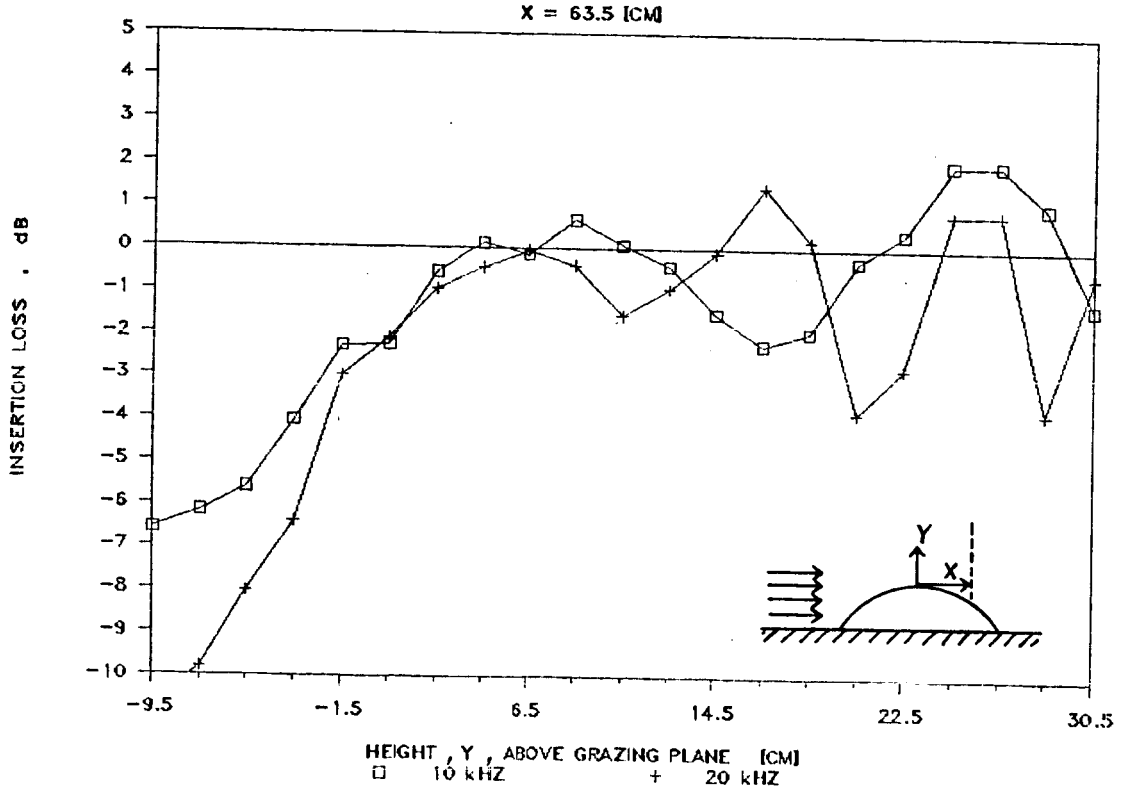

Figure 14. Insertion loss as a function of height y in centimeters relative to height of top of ridge when the horizontal coordinate x is held fixed at an intermediate distance (63.5 cm) on the shadow side. The two sets of data, which for simplicity, are connected by straight lines in the plotting, correspond to frequencies of 5 kHz (□) and 15 kHz (+).

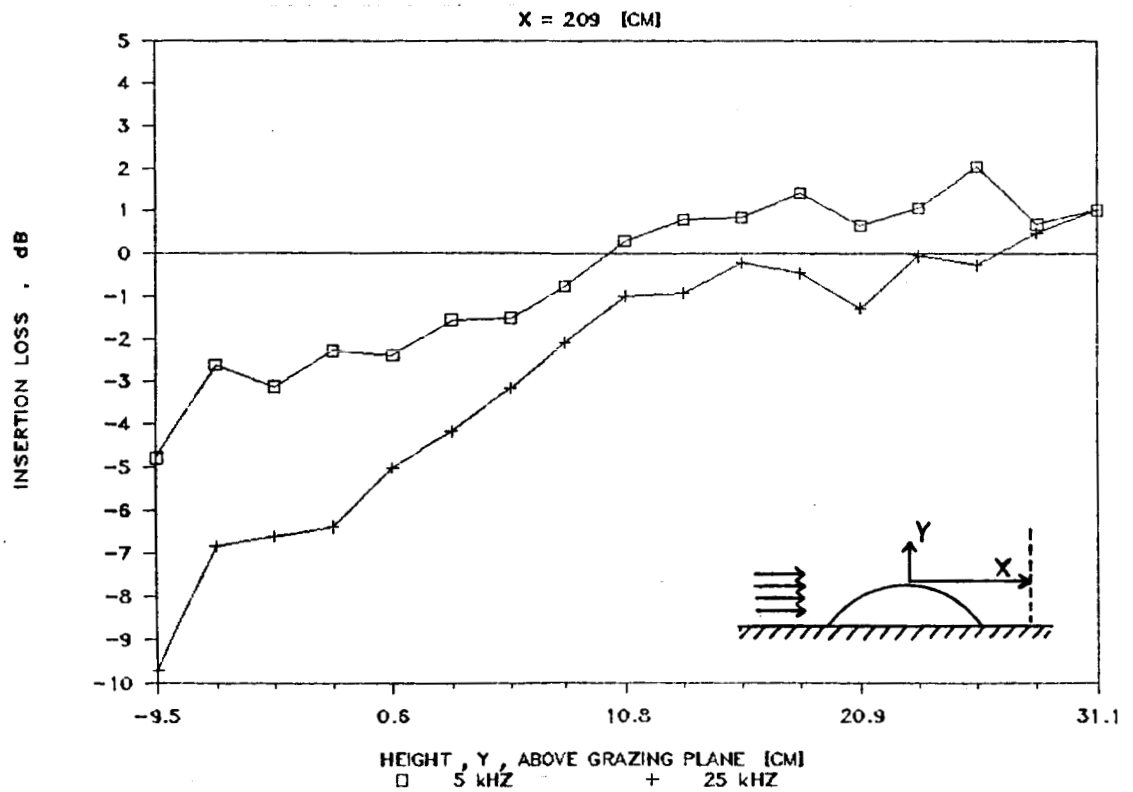

Figure 15. Insertion loss as a function of height y in centimeters relative to height of top of ridge when the horizontal coordinate x is held fixed at a relatively large distance (209 cm) on the shadow side. The two sets of data, which for simplicity, are connected by straight lines in the plotting, correspond to frequencies of 5 kHz (□) and 15 kHz (+).

ANALYTICAL STUDIES

Successful application of theoretical acoustics to outdoor propagation over undulating terrain is in principle possible, but presents challenges. The authors' considerations are presently limited to when the terrain is slowly varying over distances comparable to a wavelength; many realistic outdoor situations should be well-modelled without violation of such a restriction. The overall hope is that asymptotic and matching techniques can enable one to splice together mathematical models for intricate circumstances (such as multiple undulations) from those for simpler circumstances.

Discussion of the Echo Problem

Another key element in the research program currently in progress is the understanding of echoes from terrain. The theory is relatively simple if the echoes correspond to rays of sound that are specularly (angle of incidence equals angle of reflection) reflected from a surface, but it is likely that one may have echoes in circumstances where no such ray exists. Ordinarily, one might regard echoes as being of minor importance, but there are situations where the dominant arriving sound from a distant source could actually appear to be arriving from a direction opposite to that of the source.

Figure 16 describes such a situation: the microphone or listener is in a valley between two ridges. The source is some distance ahead of the ridge in front of the listener, and the ridge behind the listener is higher than the one in front. The geometry is such that the farther ridge is not shadowed from the source by the nearer ridge. Consequently, sound can reach the listener either as (i) a wave diffracted around the nearer ridge, or (ii) as a wave that has "echoed off" the ridge behind. Because the diffracted wave is intrinsically weak, the echo could be the stronger signal of the two.

The dominant theoretical issue that must be resolved before echoes are incorporated into the theory is what are the amplitudes associated with received non-specularly reflected echoes. To resolve this issue, Allan Pierce is presently examining the benchmark problem of transient narrow-band pulse echoes from a parabolic cylinder. The details of this study, at present only partly complete, will be given in a later report.

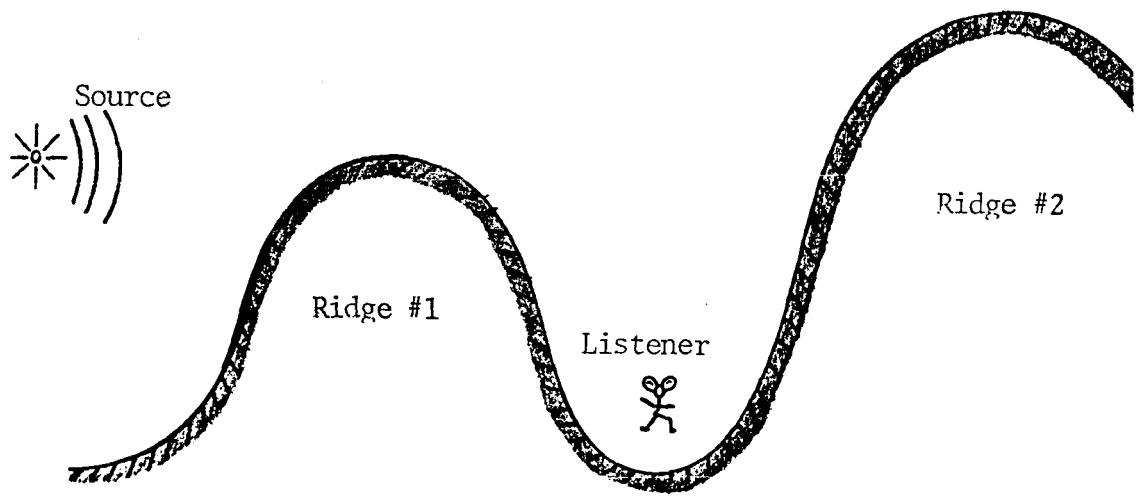

Figure 16. Sketch of circumstances in which echo from ridge behind listener may dominate over diffracted arrival over ridge between listener and source.

PAPERS AND PUBLICATIONS

The following papers will be presented at the forthcoming meeting of the Acoustical Society of America in Indianapolis, Indiana in May 1987.

Experimental investigation of the diffraction of sound by a curved surface of finite impedance. Yves H. Berthelot, James A. Kearns, Allan D. Pierce, and Geoffrey L. Main. School of Mechanical Engineering, Georgia Institute of Technology, Atlanta, Georgia 30332. —

Laboratory scale experiments have been conducted to study the diffraction of sound by a single curved ridge on top of a flat table. The sound source is an electric spark that produces a N-wave type transient of about $40\mu s$ duration. Two 1/4" microphones capture the signal at a reference position (before the ridge), and at a field point, respectively. The signals are gated to eliminate undesirable reflections, digitized (250 kHz/channel), low-pass filtered (50 kHz cut-off frequency), and processed by an IMB PC which computes the Fourier transforms of both reference and field pressure waveforms. Regardless of the spark variability, the ratio R of the Fourier transforms is constant to within 0.5 dB for the frequency range of interest (5-40 kHz). Consequently, R represents the insertion loss of the ridge as a funtion of frequency. Experimental results include, for two different surface impedances, (1) the insertion loss on the curved surface, and (2) the diffraction pattern in the transition region between the illuminated and shadow zones (penumbra), measured at an horizontal distance of 0 m, 0.71 m, and 2.09 m from the apex of the ridge. Data will be compared with theoretical results presented earlier. [Work supported by NASA.]

Echoes from hills. Allan D. Pierce and Pei-Tai Chen. School of Mechanical Engineering, Georgia Institute of Technology, Atlanta, Georgia 30332. —

The question is raised as to whether echoes from hills are caused by reflection, scattering, or diffraction. In a typical situation when one hears echoes from a distant hill, it is impossible to construct a geometrical acoustics path which connects source to hill to listener and yet for which angle of reflection equals angle of incidence at the hill's surface. If the hill is modeled as a trapezoid then the echoes are diffracted waves which originate at the base line (where hillside meets level ground) and at hilltop edge (where hillside meets hilltop). For hills with continuously curved surfaces, curvature radius much larger than wavelength, rigorous wedge diffraction theory is inapplicable and, moreover, the previous formulations of the geometrical theory of diffraction

by curved surfaces seem also inapplicable because they account for diffraction effects only on the shadow side. Recent work by Medwin and others suggests also that the validity of physical optics approximations is questionable. In an attempt to understand the general physics of hill echoes, the authors have studied the classic rigorous solution for CW plane wave incident on a hard parabolic cylinder. The contour integral with Whittaker functions in the integrand is approximated in the high frequency limit for remote points back toward the source. [Work supported by NASA Langley Research Center.]

The paper, whose abstract follows below, is an ***invited paper*** and will be presented at the forthcoming NOISE-CON meeting sponsored by the Institute of Noise Control Engineers at the Pennsylvania State University in June 1987. A preprint of this paper, prepared to meet a February 1, 1987 deadline and consequently less complete that what will actually be presented, is included in this report as an appendix.

Diffraction of Sound by a Smooth Ridge. Yves H. Berthelot, Allan D. Pierce, James A. Kearns, and Geoffrey L. Main. School of Mechanical Engineering, Georgia Institute of Technology, Atlanta, Georgia 30332. —

Laboratory scale experiments have been conducted to study sound propagation over a single curved ridge on top of a flat table. The sound source is an electric spark that produces an N-wave type transient of about 40 μs duration. Two 1/4 in. microphones capture the signal at a reference position (unaffected by the ridge), and at a field point, respectively. The signals are gated to eliminate undesirable reflections, digitized (250 kHz), low-pass filtered (50 kHz cut off frequency), and processed by an IBM PC which computes the Fourier transforms of both reference and field pressure waveforms. The ratio R of the Fourier of the Fourier transforms of the signals is independent of the spark signature to within 0.5 dB for the frequency range of interest. Consequently, R can be interpreted as the insertion loss of the ridge as a function of frequency. Experimental results include insertion loss on the surface of the ridge and behind the ridge, in the penumbra region. [Work supported by NASA Langley Research Center].

REFERENCES

[1] Semiannual Status Report No. 1, NASA Grant NAG-1-566, Georgia Institute of Technology, Atlanta, September 1985.

[2] Semiannual Status Report No. 2, NASA Grant NAG-1-566, Georgia Institute of Technology, Atlanta, February 1986.

[3] Semiannual Status Report No. 3, NASA Grant NAG-1-566, Georgia Institute of Technology, Atlanta, August 1987.

[4] M. Almgren, Scale model simulation of sound propagation considering sound speed gradients and acoustic boundary layers at a rigid surface, Report F86-05, Chalmers University of Technology, (Göteborg, Sweden, 1986).

APPENDIX

Appended here is the preprint of the paper that will be presented at the forthcoming NOISE-CON meeting at Pennsylvania State University in May, 1987.

DIFFRACTION OF SOUND BY A SMOOTH RIDGE

Yves H. Berthelot, Allan D. Pierce, James A. Kearns, and Geoffrey L. Main

The George W. Woodruff School of Mechanical Engineering,
Georgia Institute of Technology, Atlanta, Georgia 30332 USA

The objective of this research is to understand the propagation of sound over uneven terrain and irregular topography. The interest of this study focuses on circumstances where the acoustic propagation is similar to what might be expected from air vehicles flying at low altitudes, such that rays from the source arrive at angles close to grazing incidence. In general, irregular topography greatly complicates the task of predicting the acoustic field at low altitudes. It is anticipated, however, that the method of matched asymptotic expansions can be successfully applied to a wide variety of geometries, provided that the terrain is slowly varying over distances comparable to a wavelength. As a first attempt toward the analysis of more complicated geometries, the diffraction of sound by a single smooth ridge is studied both theoretically and experimentally.

A theory based on the work of Fock [1] for the diffraction of electromagnetic waves has been recently presented [4]; it does corroborate the results of Keller [2] and Hayek *et al.* [3] and yields predictions for the pressure field around a single smooth ridge, on the surface (inner region), in the shadow zone (creeping wave region), and in the penumbra region (transition between the illuminated and the shadow zone.)

The present article concerns laboratory scale experiments that have been conducted to study the diffraction of sound by a simple curved ridge. Experimental results include the insertion loss on the curved diffracting surface, and in the penumbra region, at several distances from the apex of the ridge.

EXPERIMENTAL APPARATUS

Laboratory scale experiments are being conducted on a 4.88 m by 2.44 m (16 ft by 8 ft) plywood bench top with a cylindrical ridge whose radius of curvature is about 2.5 m ($\sim$ 8 ft). A block diagram of the experiment is shown in Figure 1. Because of the semi-reverberant nature of the room, it is not practical to use a continuous sound source. Instead, an electric spark is used to produce a short transient. Frequency dependence of the parameters of importance (such as impedance, insertion loss, etc...) is obtained by means of Fourier transforms. The electric spark is generated by a high voltage (typically 2 kV) across two electrodes separated by a 1 mm gap. As in the design of Almgren [5], the spark is triggered by a third (low power) electrode placed between the two high power electrodes. The result is a 42 ± 2 μs duration pressure signal that resembles an N-wave with an amplitude of typically 150 Pa at 1 m, and whose frequency spectrum is quite broad and smooth with a maximum around 25 kHz. Although the spark source is much more repeatable than anticipated, the experimental procedure does not rely on the consistency between consecutive sparks. Two 1/4-in (B&K 4136) microphones capture the signal at a reference position (unaffected by the ridge), and at a variable field point, respectively. The ratio of the Fourier transforms of the field and reference pressures is independent of the spark signature to within 1 dB between 4 and 8 kHz, and to within 0.5 dB between 8 and 40 kHz. Consequently, the ratio of the Fourier transforms, corrected by the spherical spreading between the two microphones, can be interpreted as the insertion loss as a function of frequency, at a given field point.

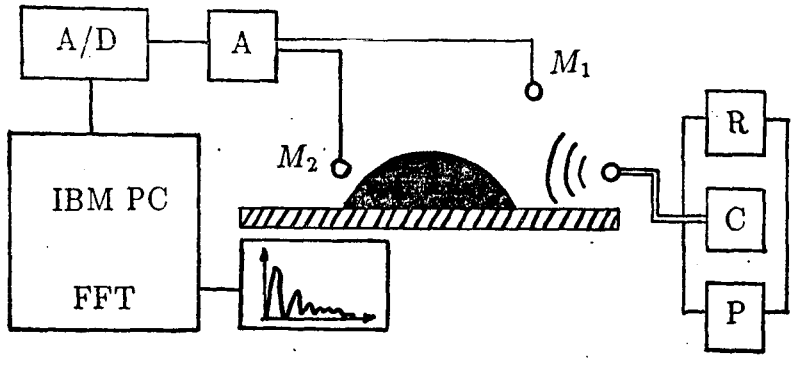

Figure 1: Block diagram of the experiment. Spark source (S) includes power supply (P), resistor (R), and capacitor (C); signals from reference microphone (M_1) and field microphone (M_2) are amplified (A), digitized (A/D), and processed by the IBM PC/XT.

The signals recorded by the microphones are amplified and digitized (250 kHz sampling rate). An IBM PC/AT with an ISC A/D converter serves as a digital oscilloscope and spectrum analyzer. The signals are digitally filtered (cut-off frequency of 50 kHz) and undesirable reflections are eliminated by appropriate gating of the signals. Fourier analysis is performed by a standard FFT algorithm with no window applied to the waveform because spectral leakage was found to be unsignificant in the transformed signals. The source directivity in a vertical plane above the bench is omnidirectional to within ± 0.5 dB, in the frequency range of interest (5-40 kHz). The difference in frequency response and sensitivity between the reference and the field microphones is taken into consideration in the experimental results presented below.

INSERTION LOSS ON THE DIFFRACTING SURFACE

The apparent insertion loss along the ridge's surface is measured from $s = -50$ cm to $s = +100$ cm, where s denotes the arc length from the apex of the ridge. (s is negative in the illuminated region). The insertion loss at 5, 15, and 25 kHz is plotted in Figure 2 as a function of distance s. Qualitatively, it seems that the insertion loss follows the trend indicated by the theory [4], except for large negative values of s, where the 6 dB pressure doubling is not observed for frequencies above 5 kHz, probably because the microphone is not perfecly flushed with the ridge. Further data reduction is needed for a quantitative comparison between theory and data.

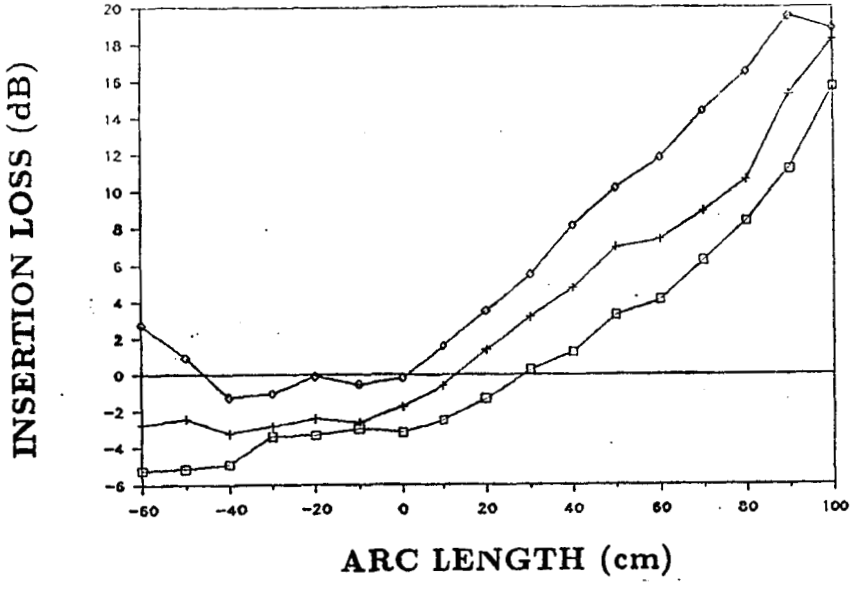

Figure 2: Insertion loss on the ridge at 5 kHz (□), 15 kHz (+), and 25 kHz (◇).

INSERTION LOSS BEHIND THE RIDGE

The diffraction of sound by the ridge is then analyzed along a vertical axis above the bench, at different distances from the source. First, the insertion loss above the apex of the ridge is shown in Figure 3 for only two frequencies (5 and 15 kHz). The abcissa in Fig. 3 is the height above the apex of the ridge. As expected from theoretical considerations, a fringe pattern occurs immediately above the ridge. Similar data is shown in Figure 4, for the diffraction pattern along the vertical axis, at a distance $s = 63.5$ cm from the apex of the ridge, (i.e., at an horizontal distance of 71 cm behind the apex of the ridge) and for 10 and 20 kHz. The abcissa in Fig. 4 is the height (in cm) over the horizontal grazing plane at the apex of the ridge. Again, experimental data seem to follow, at least qualitatively, the trends of the theoretical predictions: in the shadow region, there is no interference fringe pattern; after a smooth transition (penumbra region) toward the illuminated region, the pressure field presents an interference fringe pattern (knife-edge diffraction). Finally, the same type of experiment is performed as far as possible behind the ridge (i.e., at an horizontal distance of 2.09 m from the apex of the ridge); the acoustic pressure is measured along the vertical axis above the bench. The results are reported in Figure 5 , for frequencies of 5 and 25 kHz. As expected from physical considerations, the penumbra region seems much more important than in the data of Fig. 4.

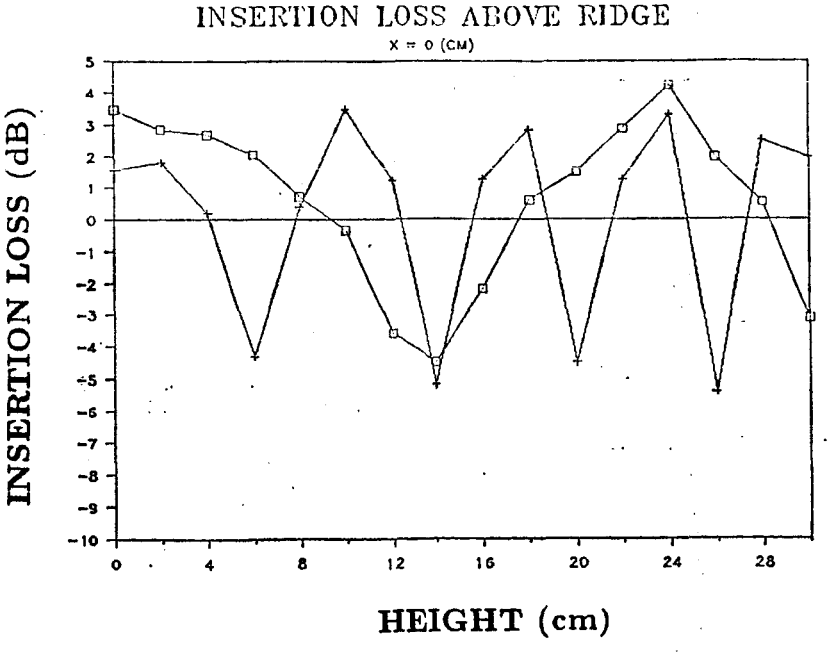

Figure 3: Insertion loss above the ridge at the apex ($x = 0$ cm) for 5 kHz ($\square$) and 15 kHz (+).

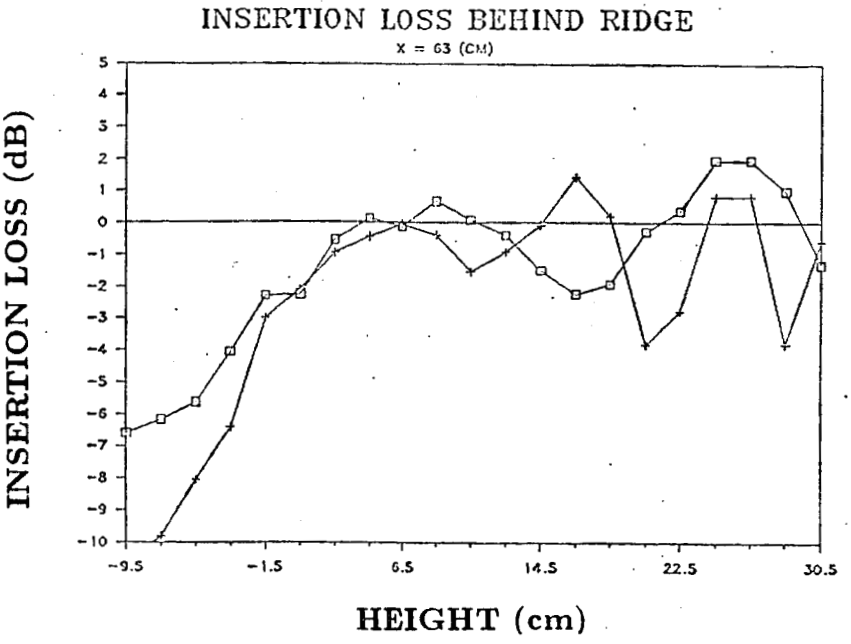

Figure 4: Insertion loss behind the ridge (x =63 cm) for 10 kHz (□) and 20 kHz (+).

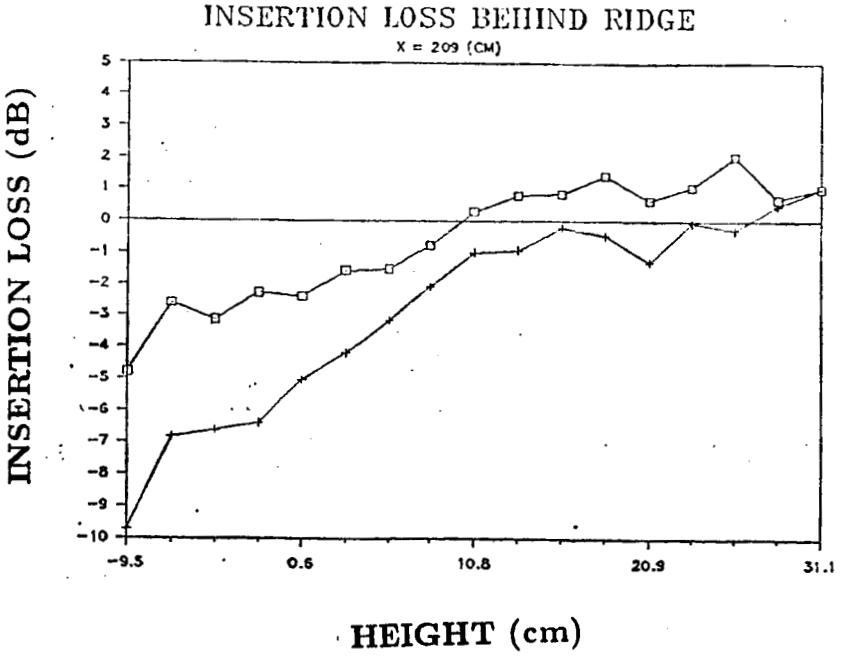

Figure 5: Insertion loss behind the ridge (x =209 cm) for 5 kHz (□) and 25 kHz (+).

CONCLUSIONS

Scale model experiments have been conducted to study the diffraction of sound by a single smooth ridge. Insertion loss measurements on the surface and behind the ridge seem to corroborate the theory of Pierce *et al.* [4], but further work is needed for a more quantitative comparison between theoretical predictions and experimental results, including an analysis on the effect of surface impedance on the insertion loss.

ACKNOWLEDGMENTS: This work was supported by NASA Langley Research Center.

REFERENCES:

1. V. A. Fock, *Electromagnetic Diffraction and Propagation Problems*, (Pergamon, London, 1965).
2. J. B. Keller, IRE Transactions on Antennas and Propagation AP-4, 312-321 (1956).
3. S. I. Hayek, *et al.*, Investigation of Selected Noise Barrier Acoustical Parameters, report to NAS-NRC Transportation Research Board, (1978).
4. A. D. Pierce, *et al.*, *Progress in Noise Control, Proceedings Inter-Noise 86*, Robert Lotz, editor, Vol. 1, pp 495-500, (Noise Control Foundation, New York, 1986).
5. M. Almgren, Scale model simulation of sound propagation considering sound speed gradients and acoustic boundary layers at a rigid surface, Report F86-05, Chalmers University of Technology, (Göteborg, Sweden, 1986).